

[Supplementary Information]

Capillary flow of amorphous metal for high performance electrode

Se Yun Kim^{1,†}, Suk Jun Kim^{1,†}, Sang Soo Jee¹, Jin Man Park¹, Keum Hwan Park¹, Sung Chan Park², Eun Ae Cho³, Jun Ho Lee³, In Yong Song³, Sang Mock Lee¹, In Taek Han¹, Ka Ram Lim^{4,‡}, Won Tae Kim⁵, Ju Cheol Park⁶, Jürgen Eckert⁷, Do Hyang Kim^{4,*} and Eun-Sung Lee^{1,*}

¹*Materials R&D Center, Samsung Advanced Institute of Technology (SAIT)*

San #14-1, Nongseo-dong, Giheung-gu, Yongin-si, Gyeonggi-do 446-712, Republic of Korea

²*Samsung SDI CO. LTD*

San #24, Nongseo-dong, Giheung-gu, Yongin-si, Gyeonggi-do 446-711, Republic of Korea

³*Computational & Analytical Science Center, Samsung Advanced Institute of Technology*

San #14-1, Nongseo-dong, Giheung-gu, Yongin-si, Gyeonggi-do 446-712, Republic of Korea

⁴*Department of Materials Science and Engineering, Yonsei University*

134 Shinchon-dong, Seodaemun-ku, Seoul, 120-749, Republic of Korea

⁵*Department of Optical Engineering, Cheongju University*

36 Naedock-dong, Cheongju, Chungbuk, 360-764, Republic of Korea

⁶*Research Institute for Advanced Materials, Seoul National University*

Kwanak-ro 599, Kwanak-gu, Seoul, 151-742, Republic of Korea

⁷*Institute for Complex Materials, IFW Dresden, P.O. Box 27 01 16, D-01171 Dresden,*

Germany and Institute of Materials Science, TU Dresden, D-01062 Dresden, Germany

[†]*These authors contributed equally to this work.*

[‡]*Present address: Light Metal Division, Korea Institute of Materials Science, 797*

Changwondaero, Seongsan-gu, Changwon, Gyeongnam 642-831, Republic of Korea

**e-mail: E.S.L., e.lee@samsung.com; D.H.K., dohkim@yonsei.ac.kr*

Supplementary Information I: Derivation of the condition for the MG to fill the cavity between Ag particles

Kumar et al. modified Hagen-Poiseuille's law to describe the nano-moulding process using metallic glass (MG)¹⁶:

$$P = \frac{32\eta}{t} \left(\frac{l}{D} \right)^2 - \frac{4\gamma \cos \theta}{D} \quad (S1)$$

Here, η is the viscosity of MG, t is the filling time of MG, l is the length of a channel, D is the diameter of the channel, γ is the surface energy of the MG, θ is the contact angle between the MG and the mould, and P is the required pressure.

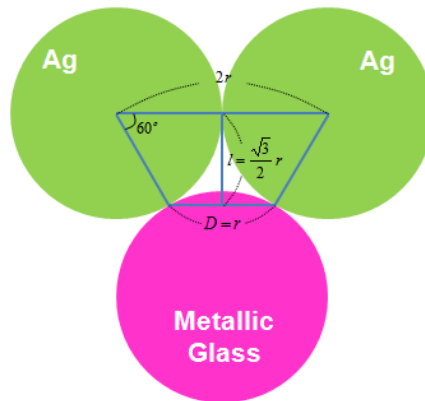
The equation (S1) suggested by Kumar et al.¹⁶ was modified to derive the condition for the MG to fill the gap between Ag particles in Ag electrode paste during the firing process. We

assumed that the aspect ratio (l/D) of the cavity between Ag particles is $\frac{\sqrt{3}}{2}$ (Supplementary

Fig. SI-1), since the length (l) of the cavity is $\frac{\sqrt{3}}{2}r$ and the diameter (D) of the cavity is r ,

while r is the radius of the Ag particles:

$$P = \frac{24\eta}{t} - \frac{4\gamma \cos \theta}{D} \quad (S2)$$



Supplementary Figure SI-1. Schematic diagram of the cavity between Ag particles. D is diameter of the channel, l is length of the channel, and r is radius of the Ag particles.

The diameter of the cavity (D) could be substituted by $d/2$, where d is the diameter of the Ag particles:

$$P = \frac{24\eta}{t} - \frac{8\gamma \cos \theta}{d} \quad (\text{S3})$$

Since there is no external pressure during the firing process, the required pressure (P) is zero:

$$0 = \frac{24\eta}{t} - \frac{8\gamma \cos \theta}{d} \quad (\text{S4})$$

The filling time (t_{fill}) of MG into the gap between Ag particles is derived as below from (S4):

$$t_{\text{fill}} = \frac{3\eta d}{\gamma \cos \theta} \quad (\text{S5})$$

Since the MG can flow effectively only in the supercooled liquid (SCL) state, the time for the MG to stay in the SCL region during the firing process, t_{SCL} , should be larger than the filling time, t_{fill} . t_{SCL} can be described as below:

$$t_{\text{SCL}} = \frac{\Delta T_x}{R_{\text{heat}}} \quad (\text{S6})$$

Here, ΔT_x is the SCL region of the MG and R_{heat} is the heating rate during the firing process.

As mentioned above, t_{fill} should be smaller than t_{SCL} for the MG to completely wet into the gap between the Ag particles:

$$t_{\text{fill}} \leq t_{\text{SCL}} \quad (\text{S7})$$

Using (S5), (S6) and (S7), the equation of the condition for the MG to fill the cavity between the Ag particles is derived as below:

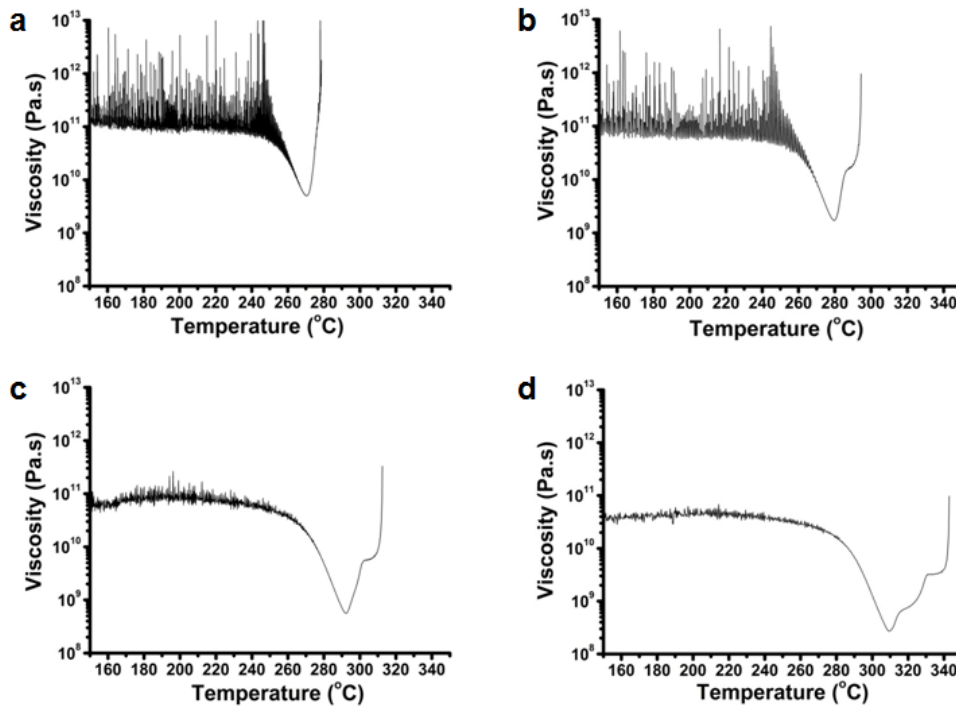
$$\frac{3\eta d}{\gamma \cos \theta} \leq \frac{\Delta T_x}{R_{\text{heat}}} \quad (\text{S8})$$

Supplementary Information II: Method for the measurement of the viscosity

Deformation rate, $d(\Delta l)/dt$, of the $\text{Al}_{85}\text{Ni}_5\text{Y}_8\text{Co}_2$ MG ribbon was measured by Thermo Mechanical Analysis (TMA) under the tensile mode at heating rates of 5, 10, 20, and 40 K/min in an Ar atmosphere. Deformation rate was divided by the length of the MG ribbon to calculate the strain, $\varepsilon=[d(\Delta l)/dt]/l$. The viscosity of the MG was derived by equation (S9).

$$\eta = \sigma / 3\varepsilon \quad (\text{S9})$$

η is the viscosity of the MG and σ is tensile stress (1 MPa). The viscosity at a heating rate of 75 K/s was evaluated by extrapolating the experimental results following the previous report which showed that the viscosity varies in proportional with the logarithmic scale of the heating rate¹⁸.

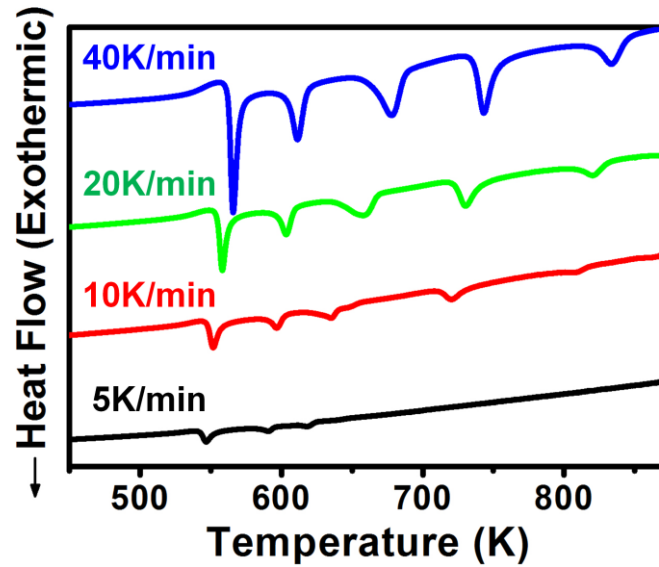


Supplementary Figure SII-1. Temperature dependence of viscosity of $\text{Al}_{85}\text{Ni}_5\text{Y}_8\text{Co}_2$ MG at heating rate of (a) 5, (b) 10, (c) 20, and (d) 40 K/min.

Supplementary Information III: Thermal properties of MG

III-1. Thermal properties of MG

Glass transition temperature (T_g), crystallization temperature (T_x) and supercooled liquid region (ΔT_x) were measured using a differential scanning calorimeter (DSC) with a heating rate of 5, 10, 20, 40 K/min in Ar atmosphere.



Supplementary Figure SIII-1. DSC curves of $\text{Al}_{85}\text{Ni}_5\text{Y}_8\text{Co}_2$ MG for various heating rate.

III-2. Prediction of T_g and T_x at heating rate of 75 K/s

To predict T_x at a heating rate of 75 K/s, Kissinger equation¹⁹ was used

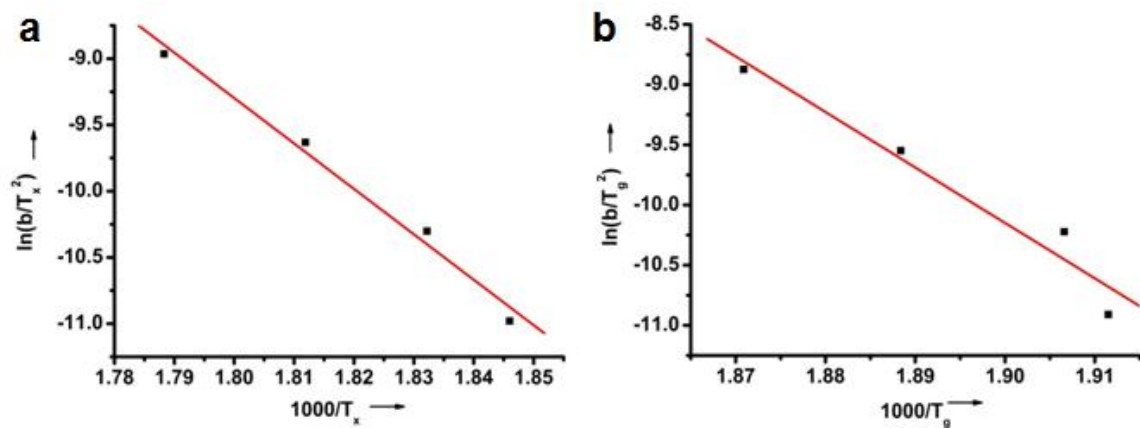
$$\ln\left(\frac{b}{T_x^2}\right) = -\frac{E_c}{RT_x} + C \quad (\text{S10})$$

b is the heating rate, E_c is an activation energy, and C is constant. Activation energy and

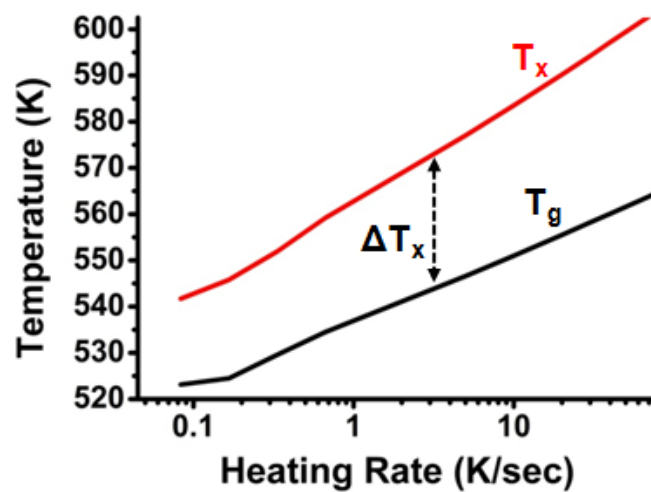
constant of crystallization were calculated by plotting $\ln\left(\frac{b}{T_x^2}\right)$ versus $\frac{1000}{T_x}$ based on T_x

values obtained at the heating rate of 5, 10, 20, 40 K/min. From the slope of the plot and y-intercept, the activation energy (E_c) and the constant were derived (Supplementary Fig. SIII-

2a). T_g at heating rate of 75 K/s was derived by same procedure as that of T_x (Supplementary Fig. SIII-2b). T_g and T_x at the heating rate of 75 K/s are 564 and 604 K, respectively, while the details of the effect of the heating rate on T_g and T_x of $\text{Al}_{85}\text{Ni}_{15}\text{Y}_8\text{Co}_2$ MG are described in Supplementary Fig. SIII-3.



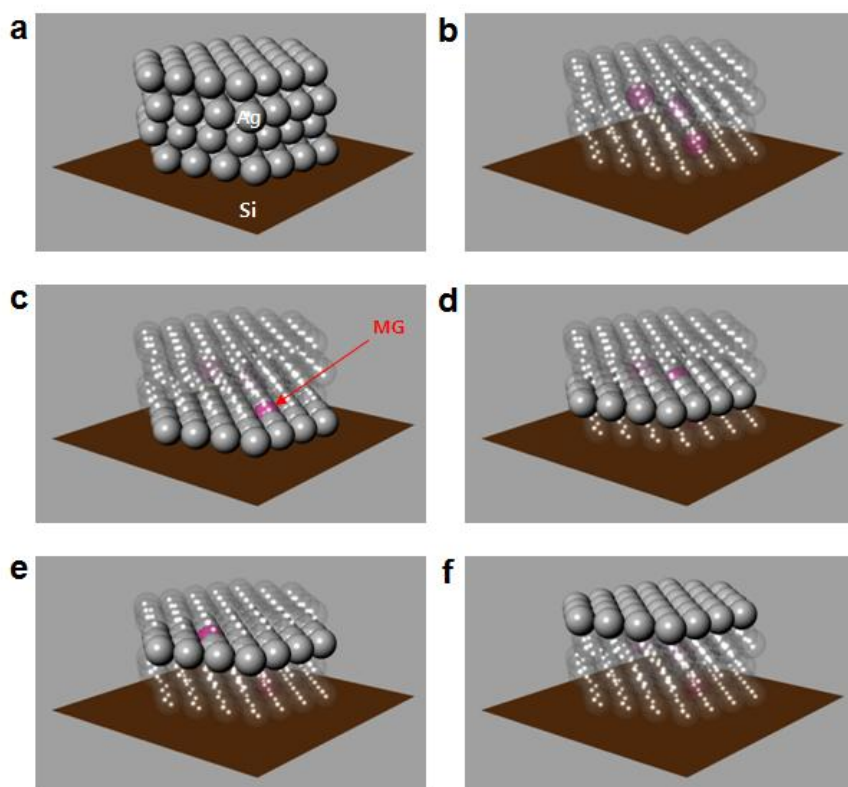
Supplementary Figure SIII-2. Kissinger plot corresponding to (a) T_x and (b) T_g in the DSC curves obtained from the $\text{Al}_{85}\text{Ni}_{15}\text{Y}_8\text{Co}_2$ MG



Supplementary Figure SIII-3. Effect of heating rate on T_g and T_x of $\text{Al}_{85}\text{Ni}_{15}\text{Y}_8\text{Co}_2$ MG.

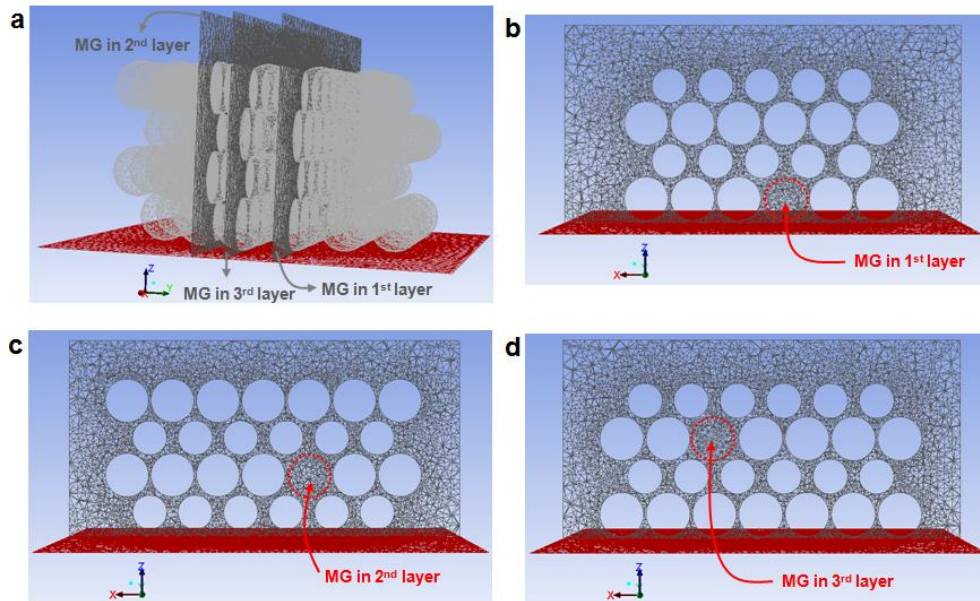
Supplementary Information IV: Simulation of the deformation behaviour of MG

The calculation system consists of 4 layers of close packed MG and Ag particles on the Si substrate. The diameter of MG and Ag particles in this system is 2 μm . Each of the first three layers from the bottom contains one MG particle and 32 Ag particles, while the fourth layer consists of only Ag particles (Supplementary Fig. SIV-1a). Each MG particle is surrounded by six of Ag particles in the first, second, and third layers from the bottom (Supplementary Fig. SIV-1a, 1b, 1c, 1d, 1e). The top layer consists of only Ag particles (Supplementary Fig. SIV-1f).



Supplementary Figure SIV-1. (a) MG/Ag paste simulation model. (b) Si substrate layer. MG particle surrounded by six of Ag particles in the (c) first, (d) second, and (e) third layers from the bottom. (f) Top layer consists of only Ag particles. Grey and red balls represent silver and MG particles, respectively. Dark brown plate is the Si substrate layer.

The computational mesh was constructed by 552,252 tetrahedral cells (Supplementary Fig. SIV-2a). Supplementary Figure SIV-2b, 2c, and 2d show the cross sections of the MG/Ag pile where the position of MG particle in each layer is indicated.



Supplementary Figure SIV-2. (a) The computational mesh of the MG/Ag pile. Cross sections of the MG/Ag pile where the MG particle is located on the (b) first layer, (c) second layer, and (d) third layer from the bottom. Light grey and dark red meshes represent silver particles and Si substrate layer, respectively.

Volume of fluid (VOF) multiphase model was applied to solve pressure-velocity coupling equation using PISO (Pressure-Implicit with Splitting of Operators) algorithm. The solution methods for gradient, pressure, momentum, and volume fraction are listed in Supplementary Table SIV-1. To control the solution convergence, the under-relaxation factors for pressure, density, body forces, momentum, and volume fraction were set as 0.3, 0.3, 0.5, 0.3 and 0.3, respectively.

Supplementary Table SIV-1. Solution methods of CFD simulation

	Solution Method
Gradient	Least Squares Cell Based
Pressure	PRESTO!
Momentum	Second Order Upwind
Volume Fraction	Second Order Upwind

The space between Ag-Ag particles and between Ag-MG particles was assumed to be filled with air with the density of 1.225 kg/m^3 and the viscosity of $1.7894 \times 10^{-5} \text{ Pa}\cdot\text{s}$.

Time step size was set to be 10^{-6} s , and 50 steps were calculated for the MG wetting simulation. Therefore, the total simulation time is 0.05 ms. In addition, the viscosity of the MG was set to be $10 \text{ Pa}\cdot\text{s}$ for this simulation. According to the equation (S11)^{S1}, the viscosity change is proportional to the elapsed wetting time.

$$R(t) = 0.65\lambda_c \left(\frac{\gamma V^3}{\eta} \right)^{0.1} (t + t_{in})^{0.1} \quad (\text{S11})$$

$R(t)$ is radius of spreading droplet, λ_c is constant, γ is interfacial tension, V is liquid volume, η is liquid viscosity, and t is spreading time. By multiplying the viscosities of the MG and the simulation time by a 10^4 factor, it was possible to investigate the deformation behavior of the MG having viscosities of $10^5 \text{ Pa}\cdot\text{s}$, while the wetting time is 0.5 s.

References

S1. Starov, V. M., Velarde, M. G. & Radke, C. J. *Wetting and Spreading Dynamics* (CRC Press, Boca Raton, FL, 2007).

Supplementary Information V: Calculation of surface tension of Al-MG and interfacial energies of MG/Ag and MG/Si.

Since the wetting capability of MG on Ag and Si is very influential in forming a good contact between the Ag electrode and the Si wafer, the contact angle of the Al-based MG on Ag and Si surface were calculated from the computational data. The contact angle is one of the indices which can estimate the wettability of the substance. Basically, to calculate the contact angle of the liquid on the solid substrate, surface tension of each phase and interfacial energy between liquid and solid phases are required. Since, it is difficult to directly measure the surface tension and interfacial energy when the MG is in the SCL state, we have performed ab initio calculations based on the density functional theory (DFT). The Vienna Ab-initio Simulation Package (VASP)^{S2} is used for DFT and molecular dynamics (MD) simulations. We carried out MD simulations to obtain the atomic structures of MG. The initial $\text{Al}_{85}\text{Ni}_{15}\text{Y}_8\text{Co}_2$ structure comprised of 200 atoms is introduced per unit supercell. The supercell was melted and equilibrated at 2000 K for 6 ps to obtain the liquid phase. The liquid phase is cooled to 200 K with a cooling rate of -400 K/ps. The density of the MG was calculated by a simple proportional method using the density data of each element in the solid state. Since the previous simulation results show the volume difference between glass and crystal of Cu-Zr alloy is approximately 2 %, the cell volume of the Al-MG was increased by 2% from that of the crystal state^{S3}. The solidified structure of MG has a cell parameter of 15.23 Å. The atomic structure of Ag was optimized using DFT simulation. The energy cutoff for the plane-wave expansion is 269.5 eV for the DFT simulation and 202.2 eV for the MD simulation. The projected-augmentedwave pseudopotential^{S4} was used to describe electron-ion interactions. Also, Perdew-Burke-Ernzerhof (PBE) functional of the generalized gradient approximation (GGA) was adopted for the exchange correlation energies between electrons^{S5}. Monkhorst-Pack^{S6} k-points are sampled on 2x2x1, 2x2x1, 2x2x2, 2x2x1, 12x12x12, and

4x4x4 meshes for MG/Ag interface, MG/Si interface, Al-MG, MG slab, Ag, and Si structures, respectively. The structures are relaxed until the maximum Hellmann-Feynman force is less than 0.02 eV/Å. Surface structures of Ag(100), Ag(110), and Ag(111) are formed to calculate interfacial energies of Ag/MG. To match the lateral periodicity, we adjust the lattice parameter of MG to that of Ag, while maintaining the same cell volume of MG. Using DFT simulation, MG/Ag interface (Supplementary Fig. SV-1a), Ag structure, and modified MG structure were optimized considering the atomic relaxation. The MG/Ag interfacial energy, $\gamma_{MG/Ag}$ is defined as:

$$\gamma_{MG/Ag} = (E_{MG/Ag} - E_{MG} - E_{Ag})/2A \quad (\text{S12})$$

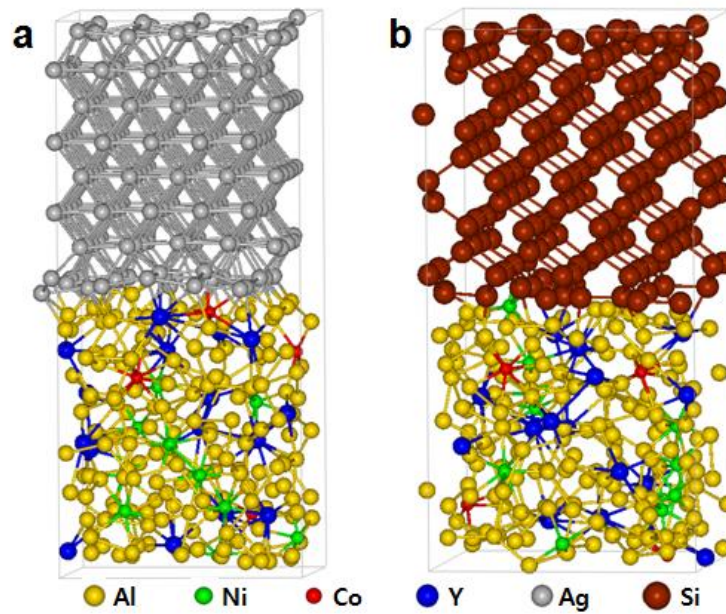
where $E_{MG/Ag}$, E_{MG} , and E_{Ag} are the total energies of MG/Ag interface, MG structure, and Ag structure, respectively. A is the area of MG/Ag interface, and the factor 2 accounts for the two interfaces in the MG/Ag cell. The MG/Si interfacial energy was calculated using the same method as that for MG/Ag case. Surface structures of Si(100), Si(110), and Si(111) were considered for calculating interfacial energies of MG/Si. To form the MG/Si interface structure, the cell parameters of MG were adjusted to match with those of Si surface structures, while maintaining the same cell volume of MG. Then, MG/Si (Supplementary Fig. SV-1b), Si, and modified MG structures are optimized using DFT simulation to calculate the MG/Si interfacial energies. The average interfacial energies of MG/Ag and MG/Si are 181.8 and 961.6 mN/m, respectively.

A single slab structure of MG separated by vacuum (20 Å) was made to calculate the surface tension of MG. The surface tension of MG, γ_{MG} is defined as:

$$\gamma_{MG} = (E_{Slab} - E_{MG})/2A \quad (\text{S13})$$

where E_{Slab} and E_{MG} are the total energies of slab MG and bulk MG, respectively. The energies of the slab structures were calculated by DFT without atomic relaxations. A is the

area of the MG slab surface, and the factor 2 accounts for the two surfaces in the MG cell. The average surface tension of MG was calculated to be 1045.7 mN/m.



Supplementary Figure SV-1. Atomic structures by DFT simulation. (a) Interface structure of $\text{Al}_{85}\text{Ni}_5\text{Y}_8\text{Co}_2$ MG with Ag. (b) Interface structure of $\text{Al}_{85}\text{Ni}_5\text{Y}_8\text{Co}_2$ MG with Si. Orange, green, red, blue, grey, and dark brown balls represent Al, Ni, Co, Y, Ag, and Si atoms, respectively.

References

- S2. Kresse, G., Marsman, M. & Furthmüller, J. VASP the GUIDE. Computational Physics, Faculty of Physics, Universität Wien. 2012. (retrieved from: <http://cms.mpi.univie.ac.at/vasp/vasp/vasp.html>)
- S3. Duan, G. *et al.* Molecular dynamics study of the binary $\text{Cu}_{46}\text{Zr}_{54}$ metallic glass motivated by experiments: Glass formation and atomic-level structure. *Phys. Rev. B* **71**, 224208-224216 (2005).
- S4. Blöchl, P. E. Projector augmented-wave method. *Phys. Rev. B* **50** 17953-17979 (1994).
- S5. Perdew, J. P., Burke, K. & Ernzerhof, M. Generalized gradient approximation made simple. *Phys. Rev. Lett.* **77**, 3865-3868 (1996).
- S6. Monkhorst, H. J. & Pack, J. D. Special points for Brillouin-zone integrations. *Phys. Rev. B* **13**, 5188-5192 (1976).

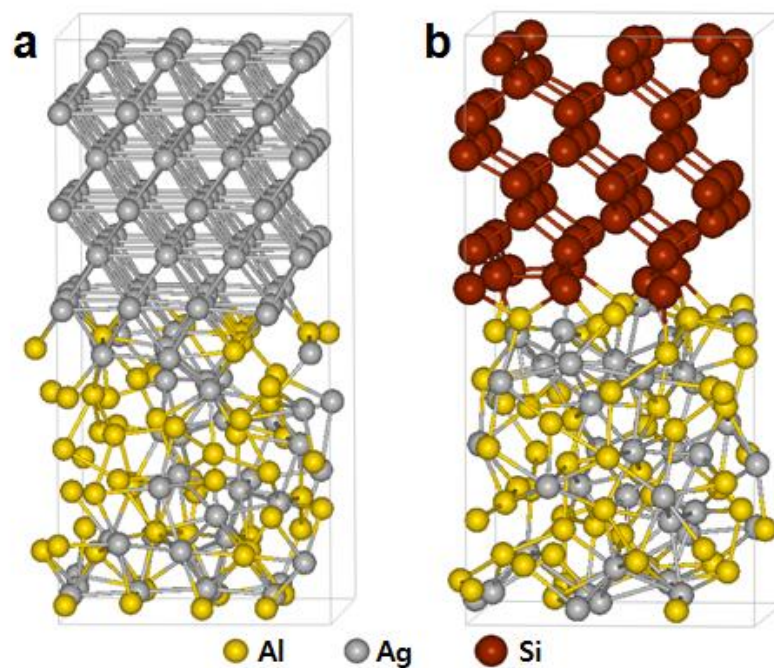
Supplementary Information VI: Interfacial energies calculation between Al-Ag eutectic and Ag, and between Al-Ag eutectic and Si by DFT simulation

The atomic structure of Al-Ag alloy was calculated by first-principles molecular dynamics calculation based on the density functional theory. Al₆₀Ag₄₀ alloy consists of 60 atoms of Al and 40 atoms of Ag in a cubic cell with periodic boundary condition, which has the cell parameter of 11.92 Å. The cell was melted and equilibrated at 2000 K for 6 ps to obtain the liquid phase. An interface structure of Al-Ag alloy/Ag is obtained by attaching the Al-Ag alloy with the Ag structure (Supplementary Fig. SVI-1a). To match the lateral periodicity, the lattice parameters of the Al-Ag alloy are adjusted to that of Ag, while the cell volume of the Al-Ag alloy is maintained. Three interfacial structure were considered; Al-Ag alloy/Ag(100), Al-Ag alloy/Ag(110), Al-Ag alloy/Ag(111). Using DFT simulation, Al-Ag alloy/Ag interface, Ag structure, and modified Al-Ag alloy structures were optimized considering the atomic relaxation. The interfacial energy of Al-Ag alloy/Ag, $\gamma_{Al-Ag/Ag}$ is defined as

$$\gamma_{Al-Ag/Ag} = (E_{Al-Ag/Ag} - E_{Al-Ag} - E_{Ag})/2A \quad (S14)$$

$E_{Al-Ag/Ag}$, E_{Al-Ag} , and E_{Ag} are the energies of Al-Ag alloy/Ag, Al-Ag alloy, and Ag structures, respectively. A is an interface area of Al-Ag alloy/Ag, and the factor 2 accounts for the two interfaces in the interface structure. An average interfacial energy of the Al-Ag alloy/Ag is -56.5 mN/m. An atomic structure and interfacial energies of Al-Ag alloy/Si interface are also calculated in a similar way as mentioned above (Supplementary Fig. SVI-1b). Three interfacial structure were considered; Al-Ag alloy/Si(100), Al-Ag alloy/Si(110), and Al-Ag alloy/Si(111). An average interfacial energy of the Al-Ag alloy/Si is 746.0 mN/m. All structures are calculated using the projected-augmented-wave pseudopotential to describe electron-ion interactions, and the energy cutoff for the plane-wave expansion is 249.6 eV for DFT simulation and 187.4 eV for MD simulation. Perdew-Burke-Ernzerhof (PBE)

functional of the generalized gradient approximation (GGA) was adopted for the exchange correlation energies between electrons. Monkhorst-Pack k-points are sampled on 2x2x1, 2x2x1, 2x2x2, 12x12x12, and 4x4x4 meshes for Al-Ag/Ag interface, Al-Ag/Si interface, Al-Ag alloy, Ag, and Si structures, respectively. The structures are relaxed until the maximum Hellmann-Feynman force is less than $0.02\text{eV}/\text{\AA}$.



Supplementary Figure SVI-1. (a) Interface structure of $\text{Al}_{60}\text{Ag}_{40}$ alloy with Ag. (b) Interface structure of $\text{Al}_{60}\text{Ag}_{40}$ alloy with Si. Orange, grey, and dark brown balls represent Al, Ag, and Si atoms, respectively.

Supplementary Information VII: Simulation of the fluidic behaviour of Al₆₀Ag₄₀ alloy

The fluidic behavior of the Al₆₀Ag₄₀ alloy in the Ag electrode was calculated using CFD simulation. Same calculation system (Supplementary Fig. SIV-1) and same computational mesh (Supplementary Fig. SIV-2) described in Supplementary Information IV were used for prediction of fluidic behavior of the Al₆₀Ag₄₀ alloy in the Ag electrode except that the MG balls are substituted by Al-Ag balls. Volume of fluid (VOF) multiphase model was applied to solve pressure-velocity coupling equation using PISO algorithm. The solution methods for gradient, pressure, momentum, and volume fraction are same as those listed in Supplementary Table SIV-1 in Supplementary Information IV. Time step size was set to be 10⁻⁵ s, and 30 steps were calculated for Al-Ag alloy flow simulation. Viscosity, density, and surface tension of the Al-Ag alloy are calculated by simple proportional method described in Supplementary Table SVII-1.

Supplementary Table SVII-1. Density, viscosity, and surface energy of Al₆₀Ag₄₀ alloy

Input parameters	Ag (Liq. 873 K) ²⁰	Al (Liq. 873 K) ²⁰	Al ₆₀ Ag ₄₀ alloy
Density (g/cm ³)	9.67	2.40	5.31
Viscosity (mPa·s)	9.65	1.45	4.73
Surface energy (mN/m)	960.7	935.0	945.3